Fog - low stratus (FLS) regimes on Corsica with wind and PBLH as key drivers

Isabel Knerr[a,*], Katja Trachte[b], Sebastian Egli[a], Johannes A.C. Barth[c], Achim Bräuning[d], Emilie Garel[e,f], Martin Häusser[d], Frédéric Huneau[e,f], Tobias R. Juhlke[c], Sébastien Santoni[e,f], Sonja Szymczak[d], Robert van Geldern[c], and Jörg Bendix[a]

[a] Philipps University Marburg, Faculty of Geography, Laboratory for Climatology and Remote Sensing, Deutschhausstr. 12, 35037 Marburg, Germany

[b] Institute for Environmental Sciences, Brandenburg University of Technology (BTU) Cottbus-Senftenberg, 03046 Cottbus, Germany

[c] Friedrich-Alexander-Universität Erlangen-Nürnberg (FAU), Department Geography and Geosciences, GeoZentrum Nordbayern, Schlossgarten 5, 91054 Erlangen, Germany

[d] Friedrich-Alexander-Universität Erlangen-Nürnberg (FAU), Department Geograpy and Geosciences, Institute of Geography, Wetterkreuz 15, 91058 Erlangen, Germany

[e] Université de Corse Pascal Paoli, Département d'Hydrogéologie, Campus Grimaldi, BP 52, 20250 Corte, France

[f] CNRS, UMR 6134 SPE, BP 52, 20250 Corte, France

* Corresponding author:
Isabel Knerr
Deutschhausstraße 12
35032 Marburg
+49 6421 28-25951
Isabel.Knerr@geo.uni-marburg.de;

Abstract: The French Mediterranean island of Corsica is already today confronted with a clear tendency towards water shortage, leading not only to socio-economical, but also to ecological problems. A potential, but not very widespread source of water is the presence of near-ground clouds, mostly fog. In this study, we investigate fog-low stratus (FLS) frequencies in Corsica, derived from a data set of Meteosat Second Generation SEVIRI, whereby a distinction between fog and low stratus is hardly feasible using remote sensing data. The FLS frequency was studied with respect to its interaction with distinct locally-generated wind and its dependence on the planetary boundary layer height (PBLH) obtained by ERA5 reanalysis (the fifth generation of the European Centre for Medium-Range Weather Forecasts, ECMWF). Results show that radiation FLS is formed in coastal areas at sunrise, with low PBLH. On the other hand, in the interior of the island at sunset, a maximum of advection FLS is formed, fostered by locally-generated and related transport of moisture. On the east side of the island, FLS frequency is lower throughout the year due to frequent lee situations. This situation is reinforced by reduced synoptic moisture transport by westerly winds, so that westerly exposed slopes benefit from moisture input by FLS formation.

Keywords: Corsica; Mediterranean; Fog Low Stratus; Meteosat Second Generation (MSG); Planetary Boundary Layer; locally-generated wind

1 Introduction

According to past measurements and future climate change projections, the French island of Corsica is already affected by climate change (Giorgi, 2006; Jacob et al., 2014). These studies projected and also observed (i) a general warming trend, whereby the monitored temperature change is up to 20% above the global average (Lionello and Scarascia, 2018), (ii) an increase in the frequency, duration and intensity of extreme weather events (IPCC, 2014), heat waves (Zittis et al., 2016), droughts (Vicente-Serrano et al., 2014), and, as a result, (iii) decreasing water resources such as reduced river discharge caused by an increase of terrestrial evapotranspiration. Particularly, the latter is assumed to increase the forest fire risk due to the extension of xeric and thermophilic ecosystems (Garbolino et al., 2015). Beyond changes in vegetation composition, another consequence of climate change will be the reduction of vegetation productivity (Gritti et al., 2006). Tree dieback can often be related to water shortage and enhanced drought stress (e.g., Choat et al., 2018; Hember et al., 2017). Although climate change is assumed to result in a general water scarcity for the Corsican society (Donta and Lange, 2008), it might be compensated by technical measures such as desalination. Such measures are, however, very costly in comparison to rain- and groundwater-fed water supply (Durham et al., 2003).

Thus, other atmospheric water sources could become important under climate change. One potential source is dew water collection, which has already been tested for Corsica (Muselli et al., 2002, 2006). Schemenauer et al. (2015) showed that the amount of collected fog water can vary between 2 and 30 l/m² per day, depending on local site conditions. Studies in the Valencia region/Spain demonstrated the high potential of fog water collection, showing satisfactory water yields (Estrela et al., 2008, 2009). However, such measures require that low clouds (Fog - low stratus - FLS) are close enough to the ground to be combed out by mesh collectors (Valiente et al., 2011; Clus et al., 2013). Therefore, knowledge of FLS frequency in several regions of Corsica is a prerequisite for an assessment of the local potential for FLS water harvesting. However, no studies on FLS occurrence in Corsica exist so far. If FLS can reach and immerse higher terrain depends on seasonal and diurnal developments of the planetary boundary layer (PBL), since in FLS situations clouds are overtopped by the PBL (Moeng, 1986; Bott et al., 1996). This also holds under high-pressure situations, when locally-generated wind (land-sea and slope breeze systems) may influence planetary boundary layer heights (PBLHs), particularly in mountainous areas such as Corsica. Land-sea breeze systems are well-described for Corsica and the neighboring island of Sardinia/Italy (Furberg et al., 2002; Metzger et al., 2014). At night, confluence of katabatic flows off the coast may even trigger deep convection rainfall (Barthlott et al., 2016). In particular, Adler and Kalthoff (2014) showed close relationships between the development of water vapor transport and PBL with several breeze systems (land-sea, mountain-valley breezes) and the topography in Corsica. Gultepe (2015) showed that the horizontal and vertical extent of fog in mountains can be very variable and may change very quickly over short time periods. Because FLS clouds are an easily visible indicator for a cloud-topped PBL (e.g. Bendix, 1994), FLS maps can also help as a surrogate of seasonal and diurnal water vapor transport that ultimately leads to FLS development.

The aims of this work are to analyze (i) spatio-temporal patterns of FLS occurrence in Corsica, (ii) impacts of the wind field on their occurrence and (iii) dependencies to the PBLH.

Corsica is a well-suited environment for this kind of investigation due to its rapid dynamics in long-term climate change and weather patterns, and because of its topographic diversity, with mountain ranges of up to 2700 m above sea level elevation.

2 Study area, data and methods

2.1 Study area and local climate

The French island of Corsica is located in the central western Mediterranean Sea between 41° 22' N and 43°01' N latitude and 8° 33' E and 9° 34' E longitude (figure 1). With a size of 8680 km² it is the fourth largest island in the Mediterranean. A central mountain ridge crosses the island from northwest to southeast. To the west of the main crest line, several smaller mountain ridges extend close to the coastline, while several valleys with a southwestern to northeastern orientation extend far inland. The eastern part of the island is characterized by a coastal plain, with valleys that also reach to the main mountain ridge. Due to its latitude and distinctive topography, the climate of Corsica is characterized by subtropical conditions with hot and dry summers in the lowlands, by temperate and wet conditions in the midlands, and by alpine conditions in the mountains. Knerr et al. (2020) showed that during 71 % of the days of the year, a large-scale situation with weak pressure gradients in the western Mediterranean prevails. This relates to radiation days and coupled land-sea-mountain breezes, which often lead to short and intense precipitation events. On the other hand, zonal circulation patterns are associated with frontal precipitation events, which mainly affect the inland part of the western side of the island. On the east side of the island, however, mainly meridional circulation patterns are responsible for intensive precipitation.

2.2 Data and methods

The basic data for this study is a data set of FLS (Fog – Low Stratus) occurrence recently derived from Meteosat Second Generation (MSG) SEVIRI data (Spinning Enhanced Visible and Infrared Imager) for the 10-year-period 2006-2015, using the retrieval scheme described in Egli et al. (2017) and Drönner et al. (2019). The method mainly relies on the emissivity difference of droplets in the 3.9 and 10 µm spectral range. It generally detects clouds with small droplet radii where detected clouds are of the FLS type (Bendix, 2002). The data set comprises binary images in 15-minute intervals for the European Domain, indicating if a pixel is covered by FLS (1) or not (0). A new dynamic threshold approach is applied in this scheme, which enables a proper classification of FLS in transition zones between daytime and nighttime hours and for variable fractions of FLS reflectance's in the 3.9. µm channel over the day. For further details, the reader may refer (Drönner et al., 2019; Egli et al., 2017)

Due to the different formation types of FLS, meteorological co-factors are needed to gain a deeper understanding of the spatio-temporal FLS distribution and frequency over Corsica. Synoptic and locally-generated wind play a decisive role in the advection of moisture to all regions of the island, and thus, for the seasonal and diurnal dynamics of FLS. In particular, wind speed is a crucial factor since it can influence FLS formation in different ways. Calm dynamics can lead to dew instead of radiation fog formation, while slow katabatic flows can enhance ground FLS formation. In contrast, higher locally-generated- or synoptic scale wind speeds can lead to turbulent suppression or dissipation of FLS, or to the uplift of the base of ground fog layers. This is often associated with slope advection and higher wind speeds in an inversion-topped PBL that can lead to FLS formation through forced lifting. For basic principles we refer to Bachmann and Bendix (1993) and Mason (1982). For this study, we used hourly measurements of wind speed and wind direction at meteorological stations of the Météo France network to analyze the prevailing wind and locally-generated systems, namely Ajaccio, Bastia, Solenzara, Pietralba and Sampolo.

Another co-factor for FLS is the planetary boundary layer height (PBLH), which normally limits the FLS and thus indicates an inversion. When FLS results from radiation processes, it is generally limited in its vertical extension by the PBL inversion and can serve as an easily visible indicator of PBLH. On the other hand, the development of PBLH is also a limiting factor in the formation of radiation fogs. Thus, for our analyses we used data on PBLH obtained from the ERA5 reanalysis with a spatial resolution of 0.25° by 0.25° and an hourly resolution over the time period 2006 – 2015 (Copernicus Climate Change Service (C3S), 2017). The PBLH used was averaged over an area of 0.1333° by 0.1333° (1 by 1 gridbox) around the positions of the related Météo France meteorological stations (figure 1). ERA5-PBLH data has been proven to capture the boundary layer reasonably well for studies relating PBLH dynamics with other meteorological variables (Allabakash and Lim, 2020).

The data analyses comprised the following steps. First, we cropped the FLS data set to the island of Corsica and calculated (i) annual, (ii) monthly and (iii) hourly maps of the relative FLS frequency. This was done by dividing the FLS pixel counts by the respective total number of valid time steps. We obtained the main frequencies of PBLHs by analyzing the resulting maps regarding the altitudes of seasonal and diurnal cycles of FLS occurrence. Second, we grouped the FLS frequency data in order to delineate zones with different FLS dynamics (seasonal and diurnal) by applying an unsupervised classification using the Kohonen's Self-Organizing Map (SOM) neural network algorithm with majority voting (Kohonen, 1990; Li and Ronald Eastman, 2006; Mather and Tso, 2016). The classification is based on four FLS frequency maps (0, 6, 12, 18 local solar time, LST) averaged over each month to consider both, diurnal and seasonal FLS cycles. Thus, 48 input layer neurons were used that generated 225 output layer neurons. The initial neighborhood radius was 22.21 and minimum and maximum learning rates are set to 0.5 and 1, respectively. We used every third column and seventh row for training the neural network. The k-means cluster algorithm (Jain, 2010) was applied to organize competitive output layer neurons into the final clusters of spatial FLS types. We iterated with classifications allowing for a maximum of 5 to 20 clusters in order to minimize the quantization error (QE) for finding the best-matching model. We finally selected the run with a maximum allowance of 16 clusters. This yielded seven clusters after 286 iterations with a QE of 0.017. The analysis delivers an interpretation of the FLS occurrence within each cluster.

We subsequently analyzed the co-factor data (wind field and PBLH) to relate them to FLS dynamics and spatial FLS clusters. Regarding the co-factor wind, we discriminated between the potential influence of diurnal locally-generated wind and synoptic scale circulations. To determine days with predominant locally-generated wind, the method outlined in Knerr et al. (2020) was applied. This is based on the assumption that the wind blows onshore / upslope (offshore / downslope) for at least 9 hours during the day (at night). An additional pre-requisite was that of the total 9 hours of equal wind direction, it had to keep its direction for at least two consecutive hours during the day, within a range of up to 60 degrees. The division of the wind direction into onshore/upslope and offshore/downslope was made by means of the coastline and topography at the meteorological stations. Due to the distinctive topography of the island, it is not possible to distinguish between the interacting locally-generated wind, primarily the land-sea breezes near the coast and the slope-breezes further inland, since their direction is the same and they reinforce each other, but they are combined as locally-generated wind. At the same time, synoptic or other mesoscale influences can have an impact on wind direction which may influence the presence of locally-generated wind events derived after the method of Knerr et al., 2020.

Furthermore, the method used by Furberg et al. (2002), which is generally based on an approach introduced by Borne et al. (1998), was applied to the three coastal sites of Ajaccio, Bastia and Solenzara. In addition to a change in wind direction between day and night, a temperature difference between monthly mean sea surface temperature (SST) and temperature at the climate stations (T_{land}) is considered in our study to discriminate days with and without the existence of locally-generated wind. Following Furberg et al. (2002), we calculated the temperature difference T_{land} - SST >0°C, where T_{land} is the mean temperature between sunrise and sunset. In this study, we used AVHRR Pathfinder Version 5.2 (PFV5.2) SST data, obtained from the US National Oceanographic Data Center and GHRSST (http://pathfinder.nodc.noaa.gov) where the PFV5.2 data set is an updated version of the Pathfinder Version 5.0 and 5.1 collection described in Casey et al. (2010) for SST values. The algorithm uses daytime data only while excluding all daily SST values below 8°C. Here, the monthly mean SST was calculated for the three coastal sites, with a minimum distance to the coast of 30 km and a covering area of 2.5° x 2.5° off the coast.

Comparing the two methods by Furberg et al. (2002) and Knerr et al. (2020) (results in Tab S1 and Tab. 1, respectively), there is a very good agreement with a correlation of 0.99. Only in DJF the method by Knerr et al (2020) shows a small overestimation of the breeze days. It can therefore be assumed that the formation of breeze systems on the coast is mainly favoured by wind shifts.

In addition, it is to be expected that breeze systems can form on every summer day if this is not disturbed by synoptic weather conditions. Apparently, the average frequency of Mediterranean low-pressure systems is in the range of 13% (Flocas, 1988). This suggests that a breeze system can develop on 87% of summer days. These values are in the range of the calculations according to the method of Knerr et al (2020) (see Tab. 1).

To further investigate the influence of wind speed on FLS, we distinguished days with daily average wind speeds above and below the upper (>= 3.2 m/s) and lower quartile (<= 2.1 m/s), over all stations. Wind speeds at interquartile intervals were referred to as moderate winds.

The above-ground PBLH was used as another co-factor applying linear regression. For this, we investigated the variability of the mean PBLH in the diurnal and seasonal cycle at the selected stations. Since the PBLH has a strong diurnal course, the daily maximum (minimum) values were used to calculate monthly mean daytime (nighttime) PBLH for all days within the period 2006-2015.

3 Results

3.1 Spatial distribution of Fog-Low Stratus

Figure 2 shows the mean spatial distributions of the FLS occurrences in Corsica. Highest FLS frequencies occur from November to March, with a maximum in December – February (DJF), as can be expected from the synoptic situation in the Mediterranean region. The formation of inversion layers topping FLS is favored by prolonged and weak-gradient high-pressure weather conditions, which frequently occur in the Mediterranean region (e.g. Knerr et al., 2020). These situations often occur in combination with nocturnal radiation losses, especially during DJF. The highest FLS values occurred on the western side of the island, with an average frequency of 19 % FLS occurrence over the considered time period. These areas are delimited in the east and north by mountain ranges with altitudes up to > 2700 m. In the North of the island, we found FLS frequencies of up to 18%. On the eastern coastal plain FLS frequencies of up to 13% occur in areas, which are not directly located at the coastline, but further inland.

With the onset of the warmer season (May – September), FLS frequencies decrease. In addition, areas with higher FLS frequencies are shifting from the west side towards the interior of the island. In JJA, the areas with the highest elevations in Central Corsica, as well as in the Bay of Aléria and around Bastia expose the highest values, with FLS frequencies of 7 % in June/July and 5% in August.

In SON, the FLS frequencies increase again, with values of up to 14 % in November in Central Corsica. In FSL frequencies in November are generally similar to those in March, but the coastal areas show lower values in November of around 5 %. The diurnal frequencies (figure. S.2) reveal interesting inverted frequencies, with highest FLS frequencies in winter from noon to midnight, mostly at the westerly exposed mid (12:00 LST) to higher slopes (18:00 LST). This situation is inverted at generally lower FLS frequencies in summer to a FLS maximum around sunrise in a fringe around the island at beach level. In comparison to the winter maxima in the western mid to high slopes, the summer maximum at beach level is culminating at the eastern coast.

3.2 Delineation of spatial FLS patterns

To analyze the spatial distribution of FLS occurrences and to assign them to drivers such as air mass flow directions, local flow dynamics or topographic structures, we conducted a cluster analysis applying the SOM algorithm, which resulted in seven clusters (figure 3). The largest contiguous regions of the island are covered by clusters 4 (34.7 %) and 7 (36.5 %), comprising most of the interior island area. While cluster 7 occurs mainly in the southwest of the island, restricted by the central mountain ridge in the East and in the North, cluster 4 (covering the highest elevations) extends north and east of the central mountain ridge and extends into the southeast of the island. The remaining five clusters are distributed incoherently and occupy smaller stretches of the coast and an area east of Pietralba. Clusters 2, 5 and 6, which are almost completely ~~in~~ restricted to coastal areas, show the lowest average elevations.

3.3 Mean temporal evolution of the FLS patterns

The mean annual and diurnal cycles of the FLS patterns in figures 2 and 3 obtained from the SOM analysis are shown in figures 4 and 5 and figure S1. Overall, all clusters reveal a similar annual course, with a frequency minimum in August and a peak phase during the cold months (DJF). The main difference between the annual patterns lies in percent occurrence (figure 4 and figure S1, top). It is highest in cluster 7, and lowest in cluster 1. It is also obvious that in clusters 5 and 6, the FLS frequencies in October are slightly increased compared to the other clusters occurring in the coastal areas. Furthermore, cluster 6 shows slightly higher seasonal FLS occurrences in July and September compared to clusters 2 and 5. Cluster 3 and cluster 4 show significantly higher FLS frequencies in the cold months shortly before sunrise and shortly after sunset. In addition, cluster 6 shows significantly higher FLS frequencies in MAM and JJA shortly after sunrise than the other clusters.

With regard to the diurnal cycle of FLS frequencies (figure S1, bottom), three different patterns can be identified: cluster 6 and clusters 4, 7 representing the interior area of the island, and the remaining clusters distributed in coastal areas (1-3, 5).

The coastal clusters are characterized by a clear peak in the FLS occurrence in the morning hours prior to sunrise, with mean FLS frequencies between 7.1 % (cluster 1) and 8.8 % (cluster 5) around 5 a.m. (cf. figure S1). In contrast, most minima appear during afternoon. This seems plausible because in the early morning hours, temperatures generally reach their lowest values. On the other hand, clusters 4 and 7 covering the mountainous interior of Corsica reveal only weak peaks of FLS occurrences during the morning hours of 6.5 % and 8.5 % respectively. However, all clusters show a clear minimum in the afternoon and a subsequent maximum in the early evening, which decreases during nighttime. Cluster 6 shows a different diurnal course in the percentage occurrence of FLS in Corsica. Although its peak phase occurs during the morning hours with a frequency of 9.6 % (8 am), it differs from the other clusters in terms of duration, i.e., 4 hours compared to 1 hour. This suggests that the clearance of the FLS takes considerably longer, which points to a stronger inversion near the surface. Except for some pixels, cluster 3 covers the northern and southern coastal plains, and the intra mountainous valley area east of Pietralba. Its FLS frequency is average compared to the other clusters, with two distinct maxima at sunset and sunrise, but with consistently constant higher FLS frequencies over the entire night.

3.4 Mean wind system dynamics and relations to FLS

To understand the difference of forcing conditions for FLS, which seem to be different in the western and eastern parts of the island, we analyzed the mean wind situation at meteorological stations which are also representative for the respective clusters. Since representative stations with hourly wind measurement data are not available for all clusters, only five of the original seven clusters were examined in detail. For this purpose, we used measurement data of the five available stations (figure 1) operated by Météo France, representing the western (Ajaccio), south-eastern (Solenzara) and north-eastern (Bastia) coastal areas, as well as the elevated areas in the North (Pietralba) and the South (Sampolo.

Figure 5 shows the mean daily and annual wind directions (left) and the corresponding mean wind speeds (right). Wind systems with changing directions in the diurnal cycle dominate throughout the year. They mainly differ in terms of duration concerning onshore/upslope or offshore/downslope direction, and thus strongly follow the annual cycle. At the coastal locations of Ajaccio, Bastia and Solenzara, the wind direction turns within a shorter time, whereas further inland in Pietralba and Sampolo the change of wind direction takes longer. Due to the longer period of irradiation in the summer months, the wind turns earlier (later) in the morning (evening) than in the winter months, with considerably lower velocities at all locations. In the summer months, the highest wind speeds are observed during the day when onshore/upslope winds are present, with highest velocities in Sampolo, Pietralba and Ajaccio. Due to its location at the west coast, Ajaccio is also affected by the synoptic westerly wind drift. However, this is also noticeable in Sampolo, although lower friction, which decreases with altitude, also has a less decelerating effect.

Under offshore/downslope wind conditions, especially the meteorological stations in the interior of the country show low wind speeds regardless of the month of the year. During the night hours, cold air is drained downslope with a maximum wind speed of 2 m/s. At the coastal locations, particularly in Ajaccio on the west coast, the wind speed is higher during the cold months with offshore/downslope winds occurring at night than with onshore/upslope winds during the day. However, it is striking that the dominating onshore/upslope southwest circulation is much stronger at the western coast (Ajaccio) than at the east coast (Bastia and Solenzara), while the offshore/downslope circulation (cold air drainage flow) at night ranges in the same dimension.

Table 1 shows the frequency distribution of the occurrence of locally-generated wind (based on the method described in Knerr et al. 2020) at the stations considered throughout the whole year as well as within seasons. In the interior of the island, locally-generated wind events occur on up to two-thirds of all days (Sampolo), whereas in the coastal area locally-generated winds are significantly reduced (Solenzara, about 30 %). On a seasonal basis, locally-generated wind occur on almost half of the days in the interior of the island (Pietralba and Sampolo), with lowest frequencies in DJF and SON. In JJA, most locally-generated wind occurred (56 %), while in Ajaccio on the west coast a frequency similar to that in the interior of the island was registered (89 %).

In addition, Table S1 shows the locally-generated wind occurrence percentages calculated with the modified method of Furberg et al. (2002) for the three coastal sites Ajaccio, Bastia and Solenzara.

In this study, unlike Furberg et al. (2002) and Borne et al. (1998), the SST values were taken at least 30 km from the coast in an area of 2.5° x 2.5° to best represent the thermal gradient.

To illustrate the relationship between FLS frequency, wind speed and the occurrence of prevailing locally-generated wind and non-prevailing locally generated wind, figure 6 shows this distribution for each station.

As a station in higher elevation, the type of wind (locally or non-locally-generated wind) plays a more important role at Sampolo than at the other stations. Here, at higher wind speeds, there is a higher condensation rate and thus a higher FLS frequency in the form of advection FLS. Radiation FLS, on the other hand, occurs mainly in Ajaccio on the west coast, where the FLS frequency decreases with stronger locally-generated winds. This shows that moist air is advected over the cool coast or relatively cold water and favors FLS formation.

Bastia on the east coast shows a similar behavior to Ajaccio, but in a less pronounced form due to the topography there. Here, the influence of katabatic flows is lower during strong locally-generated winds and advection are lower during humid westerly winds (non-locally-generated winds) than in Ajaccio.

In Pietralba, the influence of the topography is also evident, with its location in a valley closed off to the east and west. Here, the FLS clearly appears as a radiation or valley FLS.

In Solenzara, there are hardly any differences between locally-generated and non-locally-generated winds, with the highest FLS frequencies occurring within the strong wind-class. In both cases, this indicates advection or increased cold air drainage. Also, on the drier east coast, generally stronger katabatic winds may be needed for condensation to occur at all.

3.5 Dependence of FLS development on the PBLH

Finally, we analyzed the impact of the PBLH on FLS occurrences. This helps to distinguish (i) between an annual and daily course of the variation of PBLH at the selected stations**,** and (ii) between the daily minimum and maximum PBLHs to reflect nighttime and daytime structures in the lower troposphere.

The monthly means of the PBLH for the period 2006-2015 is illustrated in figure 7. It is obvious that in the interior of the island, in Sampolo and Pietralba, the average PBLH is higher in the warm months (571 m / 506 m) than in the cold months (approx. 260 m). In contrast, the highest average PBLHs are found in DJF at the coastal locations of Ajaccio (461 m) and Bastia (527 m), whereas in the warm months the PBLH is located at 303 m and 325 m, respectively. During DJF, when the atmosphere is well mixed due to the synoptic westerly wind drift, the PBLH in Ajaccio is higher than in the summer months, when of locally-generated wind dominate. In Solenzara on the east coast, a course similar to the other two coastal stations is observed.

At all stations, PBLH variability is lower in the summer months than in the winter months, and in autumn it is usually lower than in spring.

The diurnal course of PBLHs averaged over months and years is depicted in figure 8. All locations show the typical oscillation, with a maximum close to noon and a minimum prior to sunrise. The highest values occur at the inland stations Pietralba (1275 m) and Sampolo (1522 m). At the same time, both stations also exhibit the lowest PBLHs with 49.3 m and 52.0 m, respectively. In comparison, the coastal stations Ajaccio (west coast) and Bastia (northeast coast) have rather weak amplitude in the diurnal course, with 709 m (140 m) and 764 m (163 m). Solenzara, located further inland from the southeast coast shows an intermittent cycle.

However, differences in the variability of the PBLHs, particularly between daytime and nighttime hours, are also obvious. The three coastal stations, i.e. Ajaccio, Bastia and Solenzara, show a similar diurnal course, with a higher PBLH variability during nighttime and a clearly lower variability during the day. In Solenzara the differences in the PBLHs are less pronounced. Although also Bastia is located on the east coast too, its location is less isolated by the central mountain ridge, and thus the PBLH variability is more similar to the course at the west coast. In contrast, the two inland stations Pietralba and Sampolo reveal a higher PBLH variability during daytime but a low one during the night.

The relationship between FLS frequencies and the maximum PBLH representing daytime and the minimum PBLH indicating nighttime is illustrated in figure 9 for all locations and for the winter and summer months. Generally, a negative correlation between FLS frequencies and PBLH can be observed for winter times, while during summer a positive correlation for PBLH minimum (nighttime and early morning) is observed. During daytime this relationship is reversed.

Strongest correlation between PBLH and FLS-frequency are for the interior of the island for the summer. Here a correlation coefficient of 0.7 for nighttime and -0.6 during daytime can be observed for minimum PBLH in Sampolo, with the PBL maximum values occur mainly at midday. This can be attributed to a decrease in coastal influence and the related locally-generated wind.

For winter the correlation is highest for the coastal areas with a correlation coefficient of -0.6 in Ajaccio and Bastia, and -0.7 in Solenzara for daytime PBLH. According to a t-test all correlations are significant except inland at Sampolo station.

4 Discussion

We were able to detect different types of FLS dynamics on the island of Corsica by using a partitioning cluster analysis based on a self-organizing map (SOM) as described by Egli et al. (2019) for central Europe. Because clusters are spatially grouped on differences in diurnal and seasonal FLS frequencies, the found variances are physically related to different atmospheric forcing conditions. The lowest FLS frequencies occur in the summer months and during the day, when elevated areas are under the influence of the trade inversion, which is characterized by drier and warmer air masses (figure 2). The best conditions for FLS formation were found in the cold season and during nighttime (figure 2 and figure 4). In the coastal areas, within clusters 1, 2, 3 and 5, FLS maximum was obvious in the time just before sunrise, which indicates the occurrence of locally-generated wind from the surrounding higher mountain ranges. The peak around sunrise benefits from thermally induced turbulent mixing of relatively warm-moist air over the coastal waters with cold air of the beach fringes, leading to enhanced condensation and to the short FLS peak (figure 4). Higher variability within clusters can also be attributed to heterogeneity of the terrain (lower right panel figure 3).

Comparable phenomena were addressed by Choi and Speer (2006) for the South Korean west coast. The authors found that the prevailing synoptic westerly winds at night and the local scale wind systems compensate each other within the coastal region, so that the situation there is almost windless and a western wind regime is thus established. After sunset, cool air can condense over the coastal region due to radiation cooling, and the westerly winds also can lead to formation of advection fog.

For Corsica, similar situations can be observed in clusters 1 and 5 at the western coast. Here, FLS frequency increases slightly after sunset, whereas in other regions the frequency remains constant or decreases (figure 4). During daytime, FLS is mainly induced by diabatic processes associated with heating and mixing of the lower atmosphere. As pre-condition, humid air masses are transported either by synoptic large-scale processes or breeze systems (Knerr et al., 2020) to the respective site, enabling condensation. Compared to this behavior, synoptically sheltered basin regions in the island interior (cluster 7) show a high FLS occurrence, primarily in the hours after sunset. During the nighttime hours the intermountain basin situation likely causes a confluence of cold air drainage flow (katabatic flows) from the surrounding slopes, which feature the high FLS frequencies in this area. High FLS frequencies are also observed at midday in the west of the island (cluster 7). This shows that this region is characterized by an additional advection of westerly flow, which supports the locally-generated onshore/upslope wind circulation and leads to more intense wind circulation with higher moisture advection (e.g., Knerr et al., 2020, refer to processes of mountain and cloud venting described in Kossmann et al., 1998, 1999). The result is a daily maximum in FLS frequencies, which can be attributed to low stratus clouds. Moreover, cluster 7 exhibits high FLS frequencies throughout the day during the cold winter months (figure S1), which can be attributed to surface inversions (Cuxart et al., 2012). These authors showed for the Ebro-basin in northeastern Spain, that during the cold season the formation of radiation fog is favored. Once formed, it can last for several days.

The highest terrain elevations as well as standard deviation (figure 3) are represented by cluster 4, which is indicated by a maximum of FLS frequency after sunrise and a minimum in the afternoon hours, while the daytime hours until afternoon reveal a quasi-constant variability. The latter is caused by an increase of humidity accompanied by humidity advection with locally-generated wind as described by Adler and Kalthoff (2014). These authors showed the formation of low clouds using a cloud camera in the region around Corte, which belongs to cluster 4. The underlying mechanism causing the FLS minimum encompasses a downward transport of warm and dry air from heights around the ridge. This leads to a clearance of FLS in the afternoon in the regions east of the main ridge (Adler et al. 2016). This phenomenon also accounts for the negative correlation of the maximum PBLH in the afternoon with the FLS frequencies at stations on eastern slopes.

As illustrated in figures 6 and 9, the co-factors wind speed and development of the PBLH are key drivers of the spatio-temporal FLS patterns with local differences and effects of locally-generated winds.

High wind speeds associated with high FLS occurrences could be influenced by topographical conditions, especially inland. Here, the slopes typically induce katabatic flows when the atmosphere is calm and radiation fog develops preferentially. Shim and Lee (2017) observed comparable phenomena for two inland areas in South Korea. Strong wind speeds are a crucial factor as they are associated with higher FLS frequencies here. Large-scale synoptic situations associated with advection can transport moisture far inland, leading to the formation of FLS. This is particularly important on the west coast, which is mostly in an upwind position and where FLS are more common than on the east coast (downwind position).

One main driver for Fog-Low Stratus dynamics is wind speed. Radiation fog formation is mostly related to wind speeds < 3m/sec. Higher wind speeds facilitate promote turbulent fog clearance (e.g. Menut et al., 2014). In contrary, advection of moist air and forced convection at mountain slopes can favor fog formation also under higher wind speeds.

With respect to the co-factor PBLH as a proxy for the inversion height, a clear relationship to the FLS frequency could be demonstrated (figure 9) with differences between the locations. During the day and in summer the atmosphere is thermally expanded with a combination of locally-generated onshore/upslope wind, so that it is well mixed at high altitudes. This is reflected in the lower variability of PBLH as illustrated in figures 7 and 8.

The high significant correlations in Sampolo inland suggest this advection fog, whereas at the coastal sites the low correlation values indicate no relationship. At night, the PBLH is lower in coastal regions, but with increasing turbulent mixing in the synoptic westerly wind situation, the variability increases as well. A similar situation can be observed in winter, when the atmosphere is mixed stronger during the day when radiation increases, which in turn also increases the variability of PBLH. Here, higher significant correlation values are shown at the coastal locations and indicate the presence of radiation fog. The situation in the lee of the westerly winds can be best recognized in Solenzara, which is also located in a bay affected by sea surface temperatures. In this region the thermally-forced dynamics are stronger than in Ajaccio and Bastia, as depicted in the greater variability of the PBLH in the afternoon. Although Bastia is located on the east coast, and thus downwind of the synoptic circulation, it also shows this behavior. Presumably, the main reasons are the less isolated location by the central mountain ridge as well as the structure of the coastline, especially the bays. The latter causes converging flows which result in a higher dynamic in the lower atmosphere, depending on the strength of the locally-generated wind.

Considering the relationship between FLS frequencies and the PBLH, we found an increase of FLS with higher PBLH in coastal areas, especially on the west coast. This is mainly caused by the fact that here a deeper and thus longer lasting FLS thickness develops. However, the FLS maximum frequencies at the eastern slopes are generally lower compared to the western part. In cluster 1 on the northwest coast, the PBLH can develop less due to the steep coast, thus the nighttime cooling is lower than in flat areas on the east coast. The relatively warm water directly on the bluff increases the condensation point and thus the FLS frequency is lower than on strongly cooled areas of the coastal plain (cluster 6). As with the co-factor wind speed, this points to the effect of synoptic-scale driven westerly winds, which enhance the daily upslope transport of moist marine air mass accompanied with condensation and subsequent FLS formation. At the same time, the enhanced westerly streamflow generates lee effects at the eastern side (e.g., lee waves, see figure 10). This may restrict locally-generated wind-based FLS formation to lower altitudes. This behavior is corroborated by the PBLH development, which shows distinct, radiation and locally-generated wind conformal diurnal courses at the eastern coast, while in western Corsica, the westerly advection blurs these local effects, particularly in DJF. At the maximum PBLH an increase of the mixing depth during advection can be associated to mountain venting. In this setting the atmosphere's stratification is not stable enough to form FLS. Instead, diabatic heating and subsequently induced upslope flows and turbulent activities foster atmospheric mixing. The stronger the mixing, the fewer FLS formation can occur because they are dissolved. A summary of the occurrence of FLS is illustrated in figure 10.

This schematic diagram highlights the interaction of large and small-scale circulation as a function of the PBLH formation during daytime and nighttime together with the resulting FLS frequencies along a west-east transect between Ajaccio-Sampolo-Solenzara. Along the transect, higher FLS frequencies on the west side as well as in the interior and in valleys alternate with the lower frequencies on the east, especially directly on the slopes. The coastal areas experience more FLS as a consequence of accumulated downslope flows. These enhance the formation of FLS. The synoptic situation is influenced by divergent processes in the form of lee waves on the eastern slopes, which leads to a dissolution of FLS in these areas.

With respect to fog water collection during dry periods, Valiente et al. (2011) pointed to the high potential to reforest a mountainous region in eastern Spain with *Pinus pinaster*, among others. Szymczak et al. (2020) showed that these species are exposed to drought stress due to longer dry periods also in Corsica. Particularly the more precipitation-intensive locations on the western mountain flank experience more drought stress, since a large part of the precipitation drains on the surface, instead of infiltrating into the soil. In these regions, high FLS frequencies at the beginning of the vegetation period might counteract this drought stress. Valiente et al. (2011) showed that fog retrieval in the region around Valencia/Spain provided an average of 3.2 L/m²/day of water, which was used with further measures for reforestation of the mountain regions.

However, our FLS data set from Egli et al. (2017, 2019) do not contains information on the water content of FLS, and thus whether it would be sufficient to counteract the drought stress of the trees. Here, we would need additional retrievals of liquid water path and water profiles in the clouds as described in Lehnert et al. (2018, 2020). In order to meet the criterion of low FLS height, the PBLH must be low, which is especially fulfilled in the early morning hours. This requires not only a minimum PBLH, but also a maximum of FLS occurrences. At higher elevations, it can happen that such FLS occurrences are above the actual PBLH limit.

5 Summary and conclusion

In the present study, the spatio-temporal FLS regimes on the island of Corsica over the time period 2006-2015 as well as its driving co-factors including locally-generated wind and PBLH were investigated. In order to delineate spatial patterns and to account for local topographical properties a partitioning cluster analysis based on SOM was carried out using spatial-explicit FLS frequencies.

As driving co-factors for the FLS occurrence in the delineated clusters, the locally-generated wind encompassing wind speed as well as the PBLH could be identified. Daytime and hourly wind direction changes of five selected meteorological stations were used as an indication of locally-generated wind and were additionally divided into the three classes weak, moderate and strong.

The analysis of the FLS frequencies in general showed that the highest frequencies could be detected during DJF (up to 18 %), while JJA revealed the lowest values (up to 6 %). Overall, seven clusters were delineated, reflecting the topographical influence in terms of windward/leeward, slope and mountain-valley as well as coastal effects. FLS scenarios occurred most frequently in cluster 7, which represents the western part of the island. The reason is the proximity to the sea and an associated dominant westerly wind circulation that transports moisture to the island. This contrasts with cluster 1 on the north coast, where FLS is minimum. In the diurnal course, two FLS maxima were found: around sunrise in the cluster near the coast (FLS-frequency up to 9 %) and shortly before sunset in the interior of the island (FLS-percentage up to 14 %).

It was shown that wind speeds as well as the development of locally-generated winds have a clear influence on FLS occurrences. Particularly moderate speeds (2.1 - 3.2 m/s) and the appearance of locally-generated winds resulted in an increase of FLS. The latter is formed preferentially during MAM and JJA in dependence on the location (38 – 89 %).

In the diurnal cycle, it was revealed that advection FLS is formed during the day (correlation coefficient of –0.6) in a well-mixed atmosphere (PBLH between 1150 and 1820 m), while nocturnal FLS occurrences are mainly developed in a low PBLH ranging between 20 – 60 m in central Corsica and 35 – 185 m at the western coast. In contrast, it was shown that radiation FLS forms during the day at coastal sites in winter (correlation coefficients of -0.6 and -0.7), which disperses with increasing radiation and mixing of the atmosphere.

Furthermore we demonstrated that a stronger mixed surface layer of sufficient depth at sunrise near the coast increase FLS frequencies, which is caused by a stratified stable boundary layer. In addition, up to two hours before sunset on the other hand, a rather convective regime is established in the lower atmosphere, which prevents the formation of persistent FLS due to the instability.

In the context of the expected climate changes and increases in drought stress, we were able to show that the west coast of Corsica, with its potentially high FLS immersion, would be particularly suitable for the application of targeted irrigation with collected fog water during dry periods. However, further studies to quantify expected yield amounts are required.

Acknowledgements

The authors acknowledge Météo France and more particularly M. Patrick Rebillout from Météo France Ajaccio for supplying meteorological data. The ERA5 reanalysis data used in this study contain modified Copernicus Climate Change Service Information 2020.

Neither the European Commission nor ECMWF is responsible for any use that may be made of the Copernicus Information or the data it contains.

The Pathfinder 4km data were provided by GHRSST and the US National Oceanographic Data Center. This project was supported in part by a grant from the NOAA Climate Data Record (CDR) Program for satellites.

This project was financially supported by the German Research Foundation (DFG; grants BE1780/45-1, TR1201/2-1, GE2338/1-1, BR1895/27-1, SZ356/1-1) in the scope of the interdisciplinary research program CorsicArchive (Altitudinal Gradients and Forest Response: Climate, Hydrology and Isotope Variability of a Mediterranean Ecosystem) DFG-PAK 927/1.

Declarations of conflicts of interest: none.

References

Adler, B., Kalthoff, N., 2014. Multi-scale Transport Processes Observed in the Boundary Layer over a Mountainous Island. Boundary-Layer Meteorol. 153, 515–537. https://doi.org/10.1007/s10546-014-9957-8

Adler, B., Kalthoff, N., Kohler, M., Handwerker, J., Wieser, A., Corsmeier, U., Kottmeier, C., Lambert, D., Bock, O., 2016. The variability of water vapour and pre-convective conditions over the mountainous island of Corsica. Q. J. R. Meteorol. Soc. 142, 335–346. https://doi.org/10.1002/qj.2545

Allabakash, S., Lim, S., 2020. Climatology of planetary boundary layer height-controlling meteorological parameters over the Korean Peninsula. Remote Sens. 12. https://doi.org/10.3390/RS12162571

Bachmann, M., Bendix, J., 1993. Nebel im Alpenraum. Eine Untersuchung mit Hilfe digitaler Wettersatellitendaten. Bonner Geogr. Abhandlungen 86.

Barthlott, C., Adler, B., Kalthoff, N., Handwerker, J., Kohler, M., Wieser, A., 2016. The role of Corsica in initiating nocturnal offshore convection. Q. J. R. Meteorol. Soc. 142, 222–237. https://doi.org/10.1002/qj.2415

Bendix, J., 2002. A satellite-based climatology of fog and low-level stratus in Germany and adjacent areas. Atmos. Res. 64, 3–18. https://doi.org/https://doi.org/10.1016/S0169-8095(02)00075-3

Bendix, J., 1994. Fog climatology of the Po Valley. Riv. Meteorol. Aeronaut. 54, 25–25.

Borne, K., Chen, D., Nunez, M., 1998. A method for finding sea breeze days under stable synoptic conditions and its application to the Swedish west coast. Int. J. Climatol. 18, 901–914. https://doi.org/10.1002/(SICI)1097-0088(19980630)18:8<901::AID-JOC295>3.0.CO;2-F

Bott, A., Trautmann, T., Zdunkowski, W., 1996. A numerical model of the cloud-topped planetary boundary-layer: Radiation, turbulence and spectral microphysics in marine stratus. Q. J. R. Meteorol. Soc. 122, 635–667. https://doi.org/10.1002/qj.49712253105

Casey, K.S., Brandon, T.B., Cornillon, P., Evans, R., 2010. The Past, Present, and Future of the AVHRR Pathfinder SST Program, in: Oceanography from Space. Springer Netherlands, Dordrecht, pp. 273–287. https://doi.org/10.1007/978-90-481-8681-5_16

Choat, B., Brodribb, T.J., Brodersen, C.R., Duursma, R.A., López, R., Medlyn, B.E., 2018. Triggers of tree mortality under drought. Nature 558, 531–539. https://doi.org/10.1038/s41586-018-0240-x

Choi, H., Speer, M.S., 2006. The influence of synoptic-mesoscale winds and sea surface temperature distribution on fog formation near the Korean western peninsula. Meteorol. Appl. 13, 347. https://doi.org/10.1017/S1350482706002398

Clus, O., Lekouch, I., Muselli, M., Milimouk-Melnytchouk, I., Beysens, D., 2013. Dew, fog and rain water collectors in a village of S-Morocco (Idouasskssou). Desalin. Water Treat. 51, 4235–4238. https://doi.org/10.1080/19443994.2013.768323

Copernicus Climate Change Service (C3S), 2017. ERA5: Fifth generation of ECMWF atmospheric reanalyses of the global climate [WWW Document]. Copernicus Clim. Chang. Serv. Clim. Data Store. URL https://cds.climate.copernicus.eu/cdsapp#!/home

Cuxart, J., Cunillera, J., Jiménez, M.A., Martínez, D., Molinos, F., Palau, J.L., 2012. Study of Mesobeta Basin Flows by Remote Sensing. Boundary-Layer Meteorol. 143, 143–158. https://doi.org/10.1007/s10546-011-9655-8

Donta, A.A., Lange, M.A., 2008. Water Management on Mediterranean Islands: Pressure, Recommended Policy and Management Options 11–44. https://doi.org/10.1007/978-1-4020-6615-3_2

Drönner, J., Egli, S., Thies, B., Bendix, J., Seeger, B., 2019. FFLSD - Fast Fog and Low Stratus Detection tool for large satellite time-series. Comput. Geosci. 128, 51–59. https://doi.org/https://doi.org/10.1016/j.cageo.2019.04.003

Durham, B., Rinck-Pfeiffer, S., Guendert, D., 2003. Integrated water resource management - Through reuse and aquifer recharge. Desalination 152, 333–338. https://doi.org/10.1016/S0011-9164(02)01081-0

Egli, S., Thies, B., Bendix, J., 2019. A spatially explicit and temporally highly resolved analysis of variations in fog occurrence over Europe. Q. J. R. Meteorol. Soc. 145, 1721–1740. https://doi.org/10.1002/qj.3522

Egli, S., Thies, B., Drönner, J., Cermak, J., Bendix, J., 2017. A 10 year fog and low stratus climatology for Europe based on Meteosat Second Generation data. Q. J. R. Meteorol. Soc. 143, 530–541. https://doi.org/10.1002/qj.2941

Estrela, M.J., Valiente, J.A., Corell, D., Fuentes, D., Valdecantos, A., 2009. Prospective use of collected fog water in the restoration of degraded burned areas under dry Mediterranean conditions. Agric. For. Meteorol. 149, 1896–1906. https://doi.org/10.1016/j.agrformet.2009.06.016

Estrela, M.J., Valiente, J.A., Corell, D., Millán, M.M., 2008. Fog collection in the western Mediterranean basin (Valencia region, Spain). Atmos. Res. 87, 324–337. https://doi.org/10.1016/j.atmosres.2007.11.013

Flocas, A.A., 1988. Frontal depressions over the Mediterranean sea and central southern Europe. Les perturbations frontales au-dessus de la mer Méditerranée et de l'Europe centrale méridionale. Méditerranée 66, 43–52. https://doi.org/10.3406/medit.1988.2580

Furberg, M., Steyn, D.G., Baldi, M., 2002. The climatology of sea breezes on Sardinia. Int. J. Climatol. 22, 917–932. https://doi.org/10.1002/joc.780

Garbolino, E., Sanseverino-Godfrin, V., Hinojos-Mendoza, G., 2015. Describing and predicting of the vegetation development of Corsica due to expected climate change and its impact on forest fire risk evolution. Saf. Sci. 88, 180–186. https://doi.org/10.1016/j.ssci.2016.02.006

Giorgi, F., 2006. Climate change hot-spots. Geophys. Res. Lett. 33, 1–4. https://doi.org/10.1029/2006GL025734

Gritti, E.S., Smith, B., Sykes, M.T., 2006. Vulnerability of Mediterranean Basin ecosystems to climate change and invasion by exotic plant species. J. Biogeogr. 33, 145–157. https://doi.org/10.1111/j.1365-2699.2005.01377.x

Gultepe, I., 2015. Mountain weather: Observation and modeling, Advances in Geophysics. Elsevier Ltd. https://doi.org/10.1016/bs.agph.2015.01.001

Hember, R.A., Kurz, W.A., Coops, N.C., 2017. Relationships between individual-tree mortality and water-balance variables indicate positive trends in water stress-induced tree mortality across North America. Glob. Chang. Biol. 23, 1691–1710. https://doi.org/10.1111/gcb.13428

Jacob, D., Petersen, J., Eggert, B., Alias, A., Christensen, O.B., Bouwer, L.M., Braun, A., Colette, A., Déqué, M., Georgievski, G., Georgopoulou, E., Gobiet, A., Menut, L., Nikulin, G., Haensler, A., Hempelmann, N., Jones, C., Keuler, K., Kovats, S., Kröner, N., Kotlarski, S., Kriegsmann, A., Martin, E., van Meijgaard, E., Moseley, C., Pfeifer, S., Preuschmann, S., Radermacher, C., Radtke, K., Rechid, D., Rounsevell, M., Samuelsson, P., Somot, S., Soussana, J.F., Teichmann, C., Valentini, R., Vautard, R., Weber, B., Yiou, P., 2014. EURO-CORDEX: New high-resolution climate change projections for European impact research. Reg. Environ. Chang. 14, 563–578. https://doi.org/10.1007/s10113-013-0499-2

Jain, A.K., 2010. Data clustering: 50 years beyond K-means. Pattern Recognit. Lett. 31, 651–666. https://doi.org/10.1016/j.patrec.2009.09.011

Knerr, I., Trachte, K., Garel, E., Huneau, F., Santoni, S., Bendix, J., 2020. Partitioning of Large-Scale and Local-Scale Precipitation Events by Means of Spatio-Temporal Precipitation Regimes on Corsica. Atmosphere (Basel). 11, 417. https://doi.org/10.3390/atmos11040417

Kohonen, T., 1990. The self-organizing map. Proc. IEEE 78, 1464–1480. https://doi.org/10.1109/5.58325

Kossmann, M., Corsmeier, U., De Wekker, S., Fiedler, F., Voegtlin, R., Kalthoff, N., Guesten, H., Neininger, B., 1999. Observations of handover processes between the atmospheric boundary layer and the free troposphere over mountainous terrain. Contrib. to Atmos. Phys. 72, 329–350.

Kossmann, M., Vögtlin, R., Corsmeier, U., Vogel, B., Fiedler, F., Binder, H.J., Kalthoff, N., Beyrich, F., 1998. Aspects of the convective boundary layer structure over complex terrain. Atmos. Environ. 32, 1323–1348.

Lehnert, L.W., Thies, B., Bendix, J., 2020. A new high spatial resolution low stratus/fog retrieval for the Atacama Desert. Remote Sens. Environ. 236, 111445. https://doi.org/10.1016/j.rse.2019.111445

Lehnert, L.W., Thies, B., Trachte, K., Achilles, S., Osses, P., Baumann, K., Schmidt, J., Samolov, E., Jung, P., Leinweber, P., Karsten, U., Büdel, B., Bendix, J., 2018. A case study on fog/low stratus occurrence at las lomitas, atacama desert (Chile) as a water source for biological soil crusts. Aerosol Air Qual. Res. 18, 254–269. https://doi.org/10.4209/aaqr.2017.01.0021

Li, Z., Ronald Eastman, J., 2006. The Nature and Classification of Unlabelled Neurons in the Use of Kohonen's Self-Organizing Map for Supervised Classification. Trans. GIS 10, 599–613. https://doi.org/10.1111/j.1467-9671.2006.01014.x

Lionello, P., Scarascia, L., 2018. The relation between climate change in the Mediterranean region and global warming. Reg. Environ. Chang. 18, 1481–1493. https://doi.org/10.1007/s10113-018-1290-1

Mason, J., 1982. The Physics of Radiation Fog. J. Meteorol. Soc. Japan. Ser. II 60, 486–499. https://doi.org/10.2151/jmsj1965.60.1_486

Mather, P., Tso, B., 2016. Classification Methods for Remotely Sensed Data. CRC Press.

https://doi.org/10.1201/9781420090741

Menut, L., Mailler, S., Dupont, J.C., Haeffelin, M., Elias, T., 2014. Predictability of the Meteorological Conditions Favourable to Radiative Fog Formation During the 2011 ParisFog Campaign. Boundary-Layer Meteorol. 150, 277–297. https://doi.org/10.1007/s10546-013-9875-1

Metzger, J., Barthlott, C., Kalthoff, N., 2014. Impact of upstream flow conditions on the initiation of moist convection over the island of Corsica. Atmos. Res. 145–146, 279–296. https://doi.org/10.1016/j.atmosres.2014.04.011

Moeng, C.-H., 1986. Large-Eddy Simulation of a Stratus-Topped Boundary Layer. Part I: Structure and Budgets. J. Atmos. Sci. 43, 2886–2900. https://doi.org/10.1175/1520-0469(1986)043<2886:LESOAS>2.0.CO;2

Muselli, M., Beysens, D., Marcillat, J., Milimouk, I., Nilsson, T., Louche, A., 2002. Dew water collector for potable water in Ajaccio (Corsica Island, France). Atmos. Res. 64, 297–312. https://doi.org/10.1016/S0169-8095(02)00100-X

Muselli, M., Beysens, D., Soyeux, E., Clus, O., 2006. Is Dew Water Potable? Chemical and Biological Analyses of Dew Water in Ajaccio (Corsica Island, France). J. Environ. Qual. 35, 1812–1817. https://doi.org/10.2134/jeq2005.0357

Pachauri, R.K., Allen, M.R., Barros, V.R., Broome, J., Cramer, W., Christ, R., Church, J.A., Clarke, L., Dahe, Q., Dasgupta, P., Dubash, N.K., Edenhofer, O., Elgizouli, I., Field, C.B., Forster, P., Friedlingstein, P., Fuglestvedt, J., Gomez-Echeverri, L., Hallegatte, S., Hegerl, G., Howden, M., Jiang, K., Cisneroz, B.J., Kattsov, V., Lee, H., Mach, K.J., Marotzke, J., Mastrandrea, M.D., Meyer, L., Minx, J., Mulugetta, Y., O'Brien, K., Oppenheimer, M., Pereira, J.J., Pichs-Madruga, R., Plattner, G.-K., Pörtner, H.-O., Power, S.B., Preston, B., Ravindranath, N.H., Reisinger, A., Riahi, K., Rusticucci, M., Scholes, R., Seyboth, K., Sokona, Y., Stavins, R., Stocker, T.F., Tschakert, P., van Vuuren, D., van Ypserle, J.-P., 2014. Climate Change 2014: Synthesis Report. Contribution of Working Groups I, II and III to the Fifth Assessment Report of the Intergovernmental Panel on Climate Change. IPCC, Geneva, Switzerland.

Schemenauer, R., Gultepe, I., Witiw, M., 2015. Fog Studies. Meteorol. Technol. Int. 50–54.

Valiente, J.A., Estrela, M.J., Corell, D., Fuentes, D., Valdecantos, A., Baeza, M.J., 2011. Fog water collection and reforestation at a mountain location in a western mediterranean basin region: Air-mass origins and synoptic analysis. Erdkunde 65, 277–290. https://doi.org/10.3112/erdkunde.2011.03.05

Vicente-Serrano, S.M., Lopez-Moreno, J.I., Beguería, S., Lorenzo-Lacruz, J., Sanchez-Lorenzo, A., García-Ruiz, J.M., Azorin-Molina, C., Morán-Tejeda, E., Revuelto, J., Trigo, R., Coelho, F., Espejo, F., 2014. Evidence of increasing drought severity caused by temperature rise in southern Europe. Environ. Res. Lett. 9. https://doi.org/10.1088/1748-9326/9/4/044001

Zittis, G., Hadjinicolaou, P., Fnais, M., Lelieveld, J., 2016. Projected changes in heat wave characteristics in the eastern Mediterranean and the Middle East. Reg. Environ. Chang. 16, 1863–1876. https://doi.org/10.1007/s10113-014-0753-2

Figure 1: (a) location of the island of Corsica in the western Mediterranean (red box); and (b) terrain elevation derived from the ASTER Global Digital Elevation Model (GDEM) Version 3 (ASTGTM) of Corsica, also showing the locations of Météo France's meteorological stations (black spots) used in this study to validate FLS satellite data.

Figure 2: Spatial distribution of FLS frequency in percentage for each month of the year in Corsica, averaged over the period 2006-2015.

Figure 3: Spatial patterns of FLS frequencies (%) in Corsica using a self-organizing map classification (left), the percentage [%] of the area of the respective cluster (table, top right) and mean terrain altitude [m] per cluster with standard deviation as error bar (bottom right).

Figure 4: Isopleth diagram with annual cycle on the x-axis and diurnal cycle on the y-axis of FLS frequency [%] within clusters during the period 2006-2015.

Figure 5: Monthly and hourly averaged wind direction and wind speed during the period 2006-2015 for different meteorological stations. Wind direction was divided into 45° sectors (left).

Figure 6: Error-plot with mean and standard deviation of the prevailing locally-generated wind (red) and non-prevailing locally generated wind (grey), their intensity and the respective FLS-frequency [%], representing each month for the period 2006-2015 for each station. Lines illustrate the variation between the wind speeds. Number shows occurrences per wind class, with weak wind $\leq$ 2.1 m/s, strong wind $\geq$ 3.2 m/s and moderate in-between.

Figure 7: Monthly variation of the mean PBLH in meters above ground level for the period 2006 - 2015. Elevation of the stations: Ajaccio 5 m, Bastia 10 m, Solenzara 12 m, Pietralba 510 m, Sampolo 837 m.

Figure 8: Diurnal variation of mean PBLH in meters above ground level averaged on a monthly basis for the period 2006-2015. Elevation of the stations: Ajaccio 5 m, Bastia 10 m, Solenzara 12 m, Pietralba 510 m, Sampolo 837 m.

Figure 9: Scatterplot of the monthly mean values of the daily minimum (a) and maximum (b) PBLHs, in meters above ground level in a logarithmic scale and the respective FLS frequencies in percentage for DJF (blue) and JJA (orange). Asterisks show significance level with $p<0.05$ (*) and $p<0.01$ (**).

Figure 10: Conceptual model for explaining FLS frequencies. Maximum/minimum FLS frequencies are depicted in green/ red along a west-east transect of the island of Corsica (Ajaccio-Sampolo-Solenzara), local anabatic/onshore winds in grey and katabatic/offshore winds in black arrows, synoptic circulations (west wind circulation) in blue arrow and maximum/minimum PBLH in meters above ground level in orange/ blue dashed lines, representing the daylight and nocturnal situations

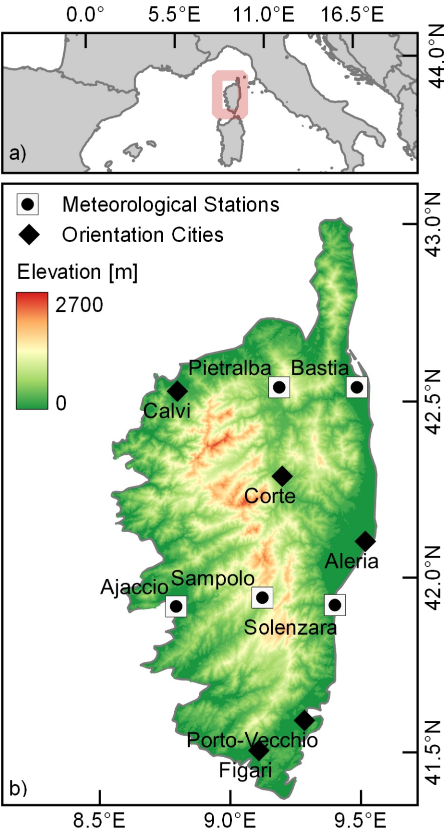
0.0°
5.5°E
11.0°E
16.5°E
44.0°N
a)
Meteorological Stations
Orientation Cities
Elevation [m]
2700
0
43.0°N
Pietralba
Bastia
Calvi
42.5°N
Corte
Aleria
42.0°N
Sampolo
Ajaccio
Solenzara
Porto-Vecchio
Figari
41.5°N
b)
8.5°E
9.0°E
9.5°E

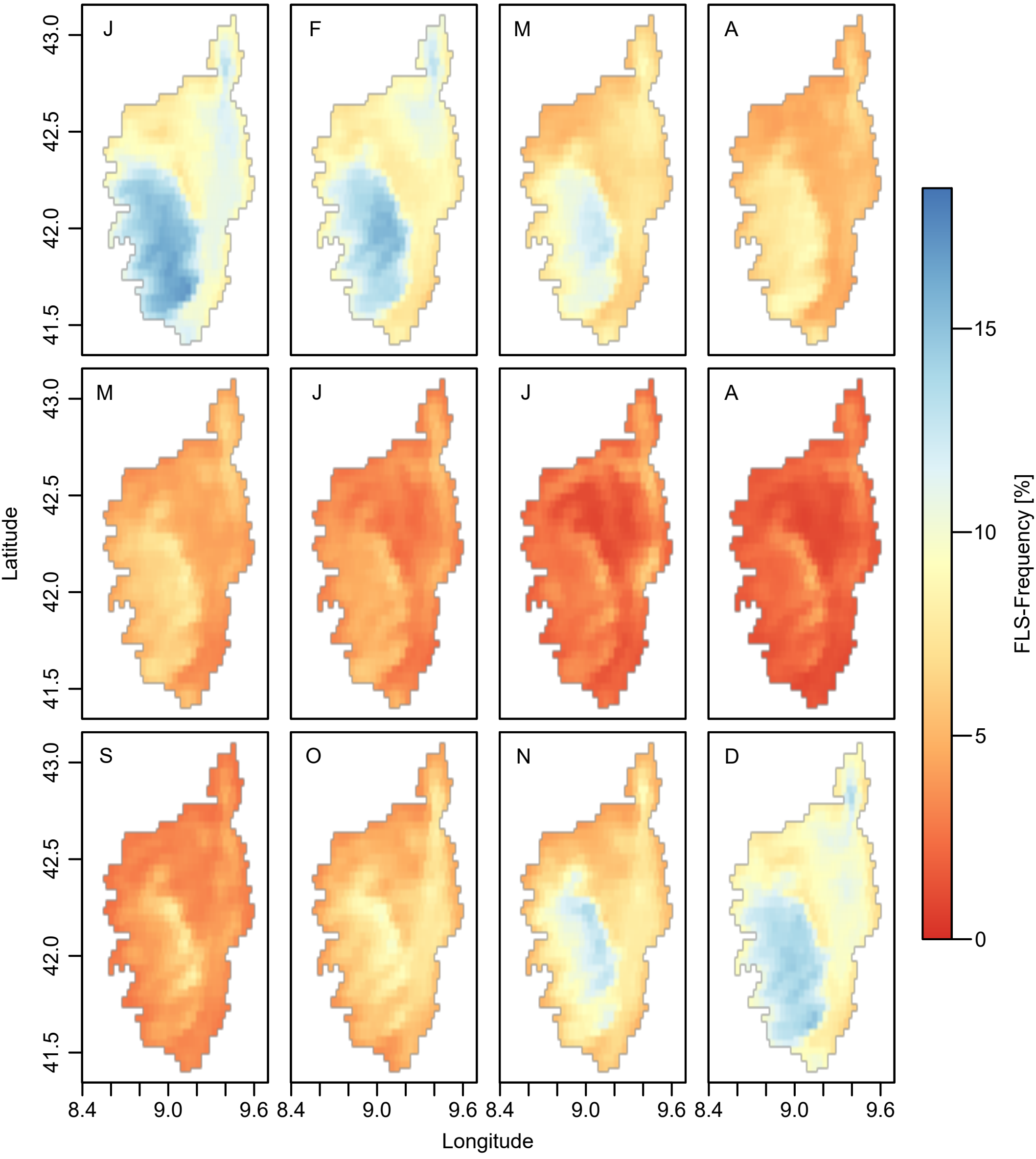

J
F
M
A
M
J
J
A
S
O
N
D
43.0
42.5
42.0
41.5
Latitude
8.4
9.0
9.6
Longitude
FLS-Frequency [%]
0
5
10
15

Cluster	1	2	3	4	5	6	7
Cover [%]	1.1	7.7	2.1	34.7	15.0	2.9	36.5

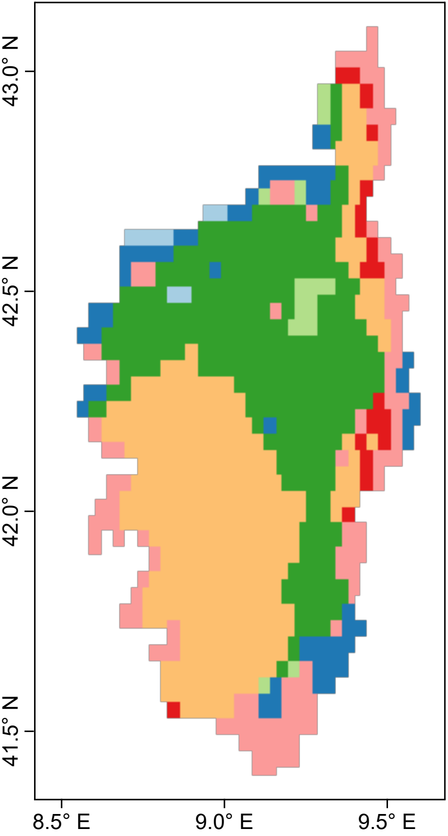

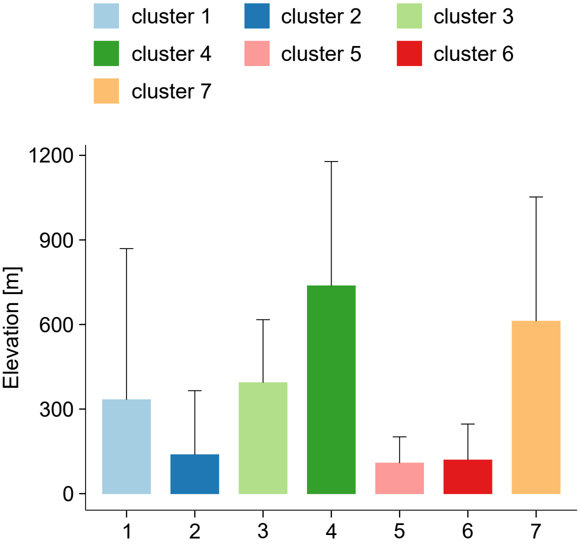

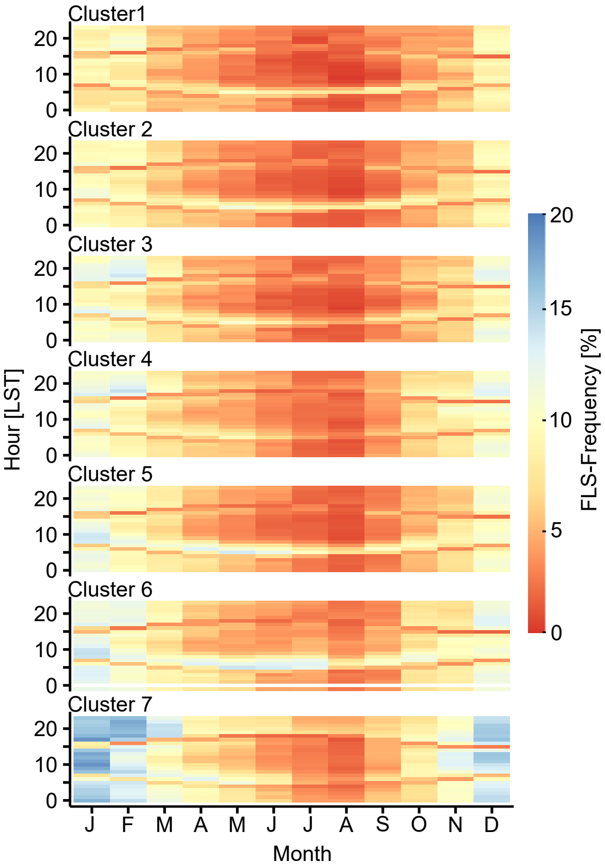

Cluster1
Cluster 2
Cluster 3
Cluster 4
Cluster 5
Cluster 6
Cluster 7
Hour [LST]
0
10
20
J
F
M
A
M
J
J
A
S
O
N
D
Month
FLS-Frequency [%]
0
5
10
15
20

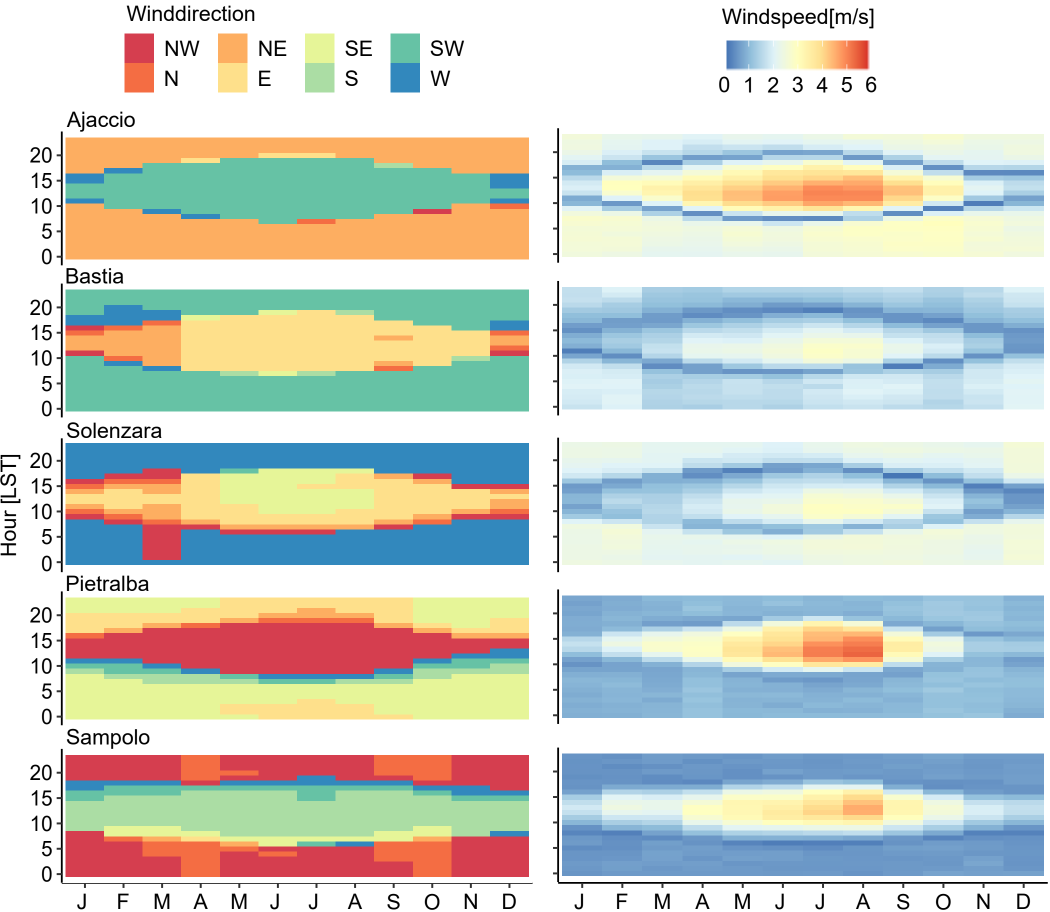
Winddirection
NW
N
NE
E
SE
S
SW
W
Windspeed[m/s]
0 1 2 3 4 5 6
Ajaccio
Bastia
Solenzara
Pietralba
Sampolo
Hour [LST]
0 5 10 15 20
J F M A M J J A S O N D

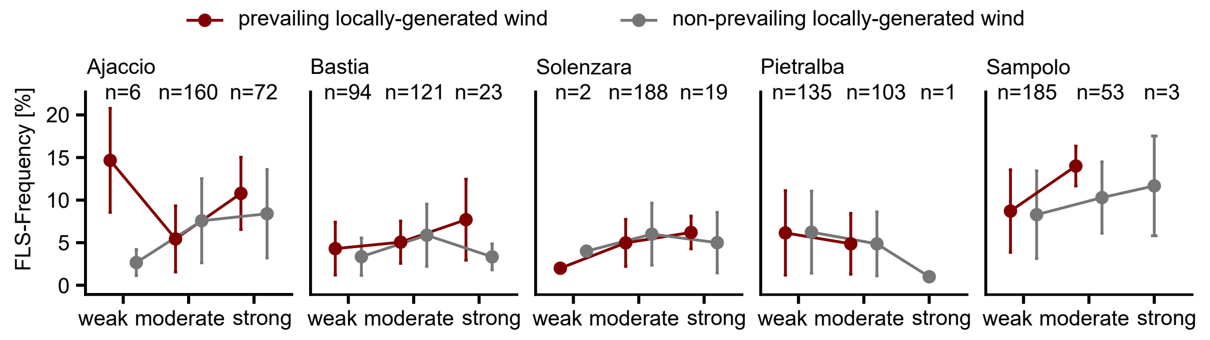
prevailing locally-generated wind
non-prevailing locally-generated wind
Ajaccio
n=6
n=160
n=72
Bastia
n=94
n=121
n=23
Solenzara
n=2
n=188
n=19
Pietralba
n=135
n=103
n=1
Sampolo
n=185
n=53
n=3
FLS-Frequency [%]
0
5
10
15
20
weak
moderate
strong

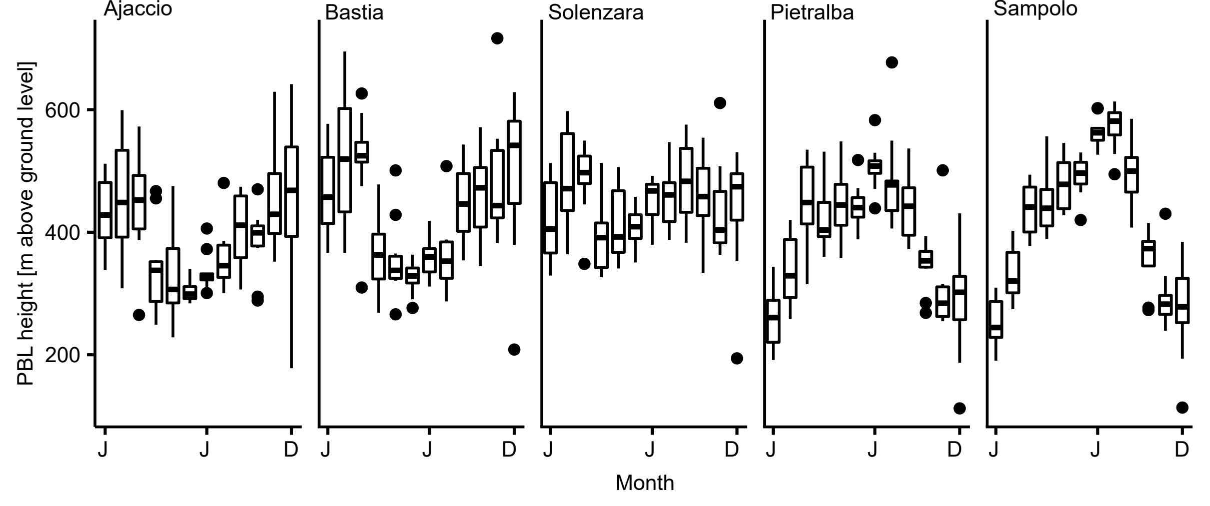
Ajaccio
Bastia
Solenzara
Pietralba
Sampolo
PBL height [m above ground level]
600
400
200
J
J
D
Month

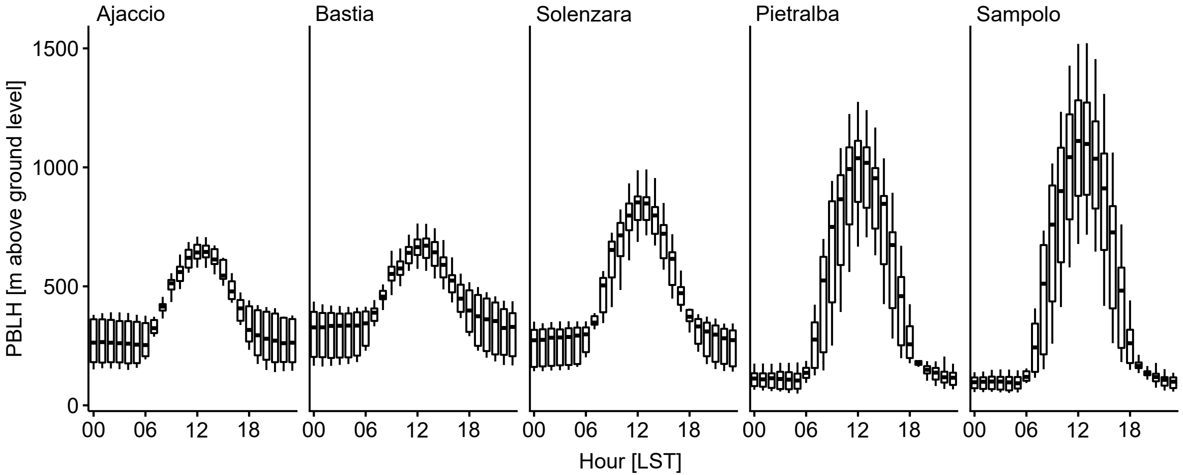

Ajaccio
Bastia
Solenzara
Pietralba
Sampolo
PBLH [m above ground level]
0
500
1000
1500
00
06
12
18
Hour [LST]

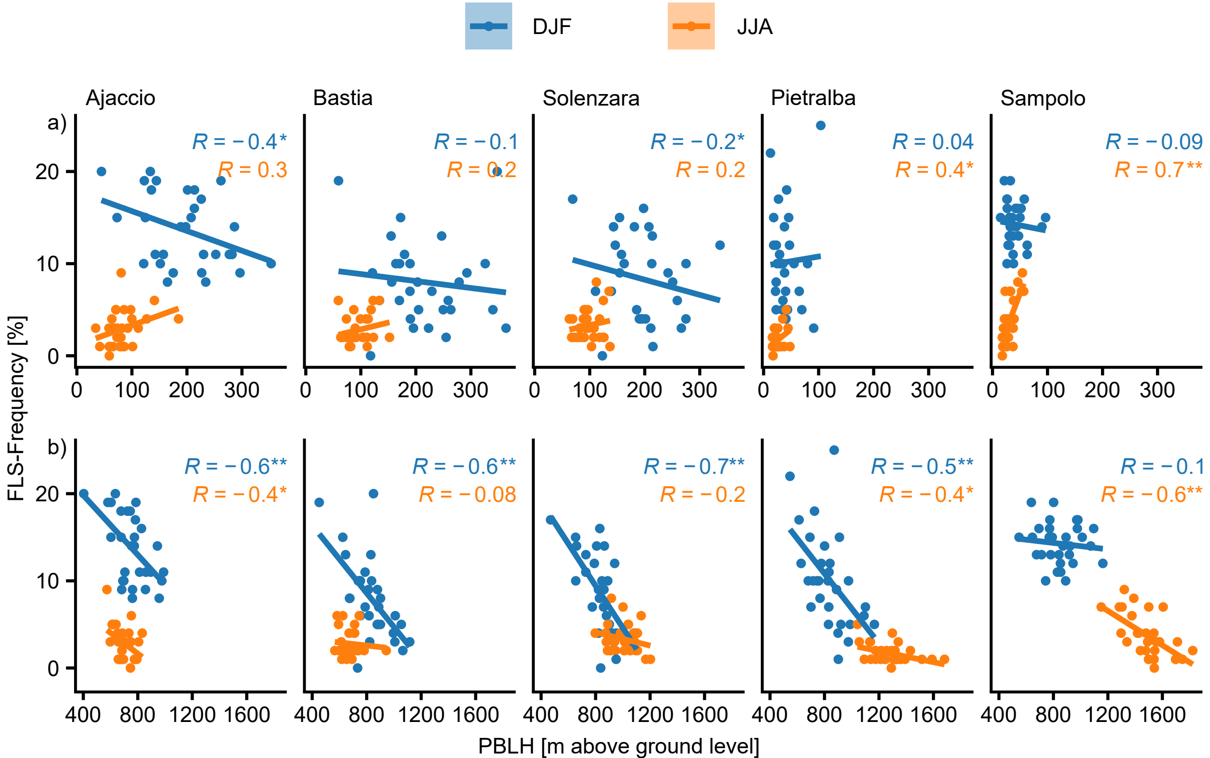
DJF
JJA
Ajaccio
Bastia
Solenzara
Pietralba
Sampolo
a)
b)
R = −0.4*
R = 0.3
R = −0.1
R = 0.2
R = −0.2*
R = 0.2
R = 0.04
R = 0.4*
R = −0.09
R = 0.7**
R = −0.6**
R = −0.4*
R = −0.6**
R = −0.08
R = −0.7**
R = −0.2
R = −0.5**
R = −0.4*
R = −0.1
R = −0.6**
FLS-Frequency [%]
PBLH [m above ground level]

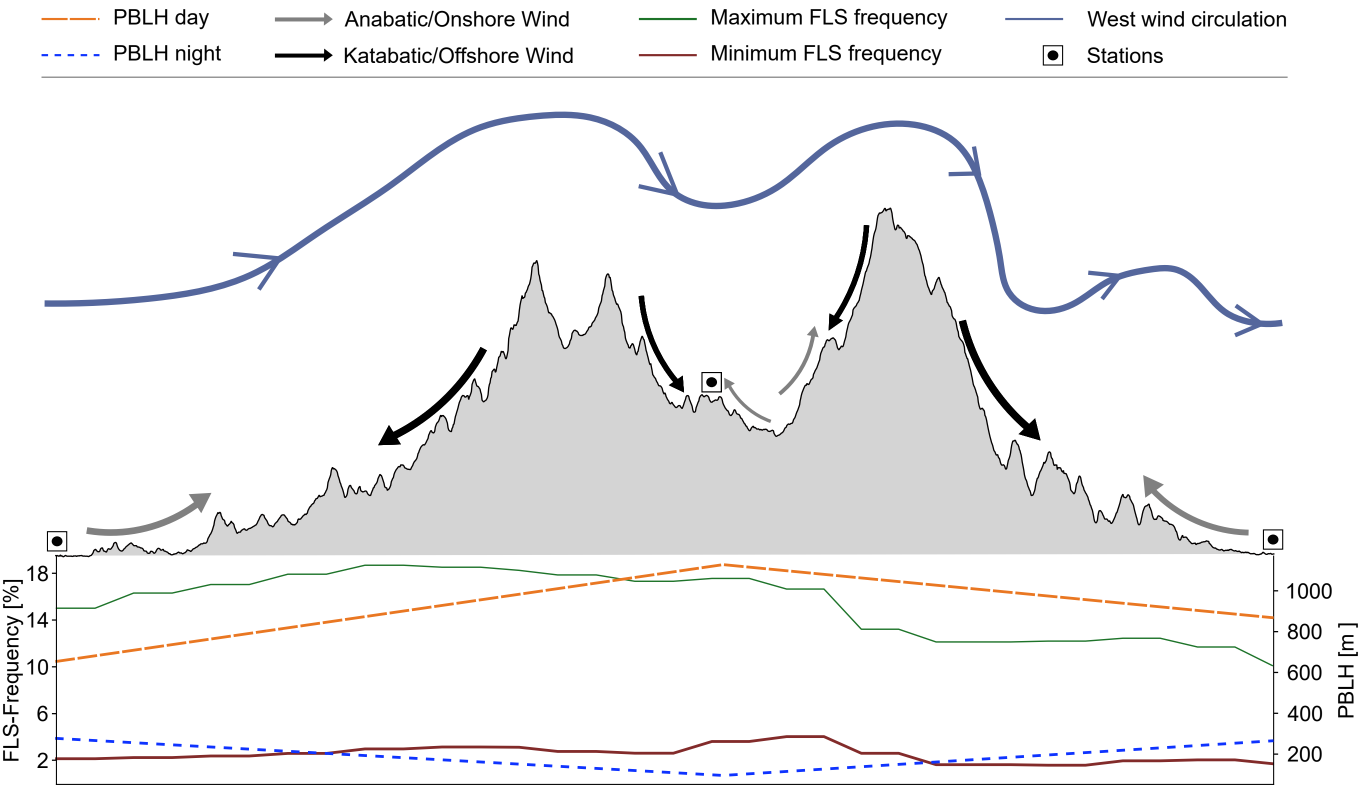
PBLH day
PBLH night
Anabatic/Onshore Wind
Katabatic/Offshore Wind
Maximum FLS frequency
Minimum FLS frequency
West wind circulation
Stations
FLS-Frequency [%]
PBLH [m]
18
14
10
6
2
1000
800
600
400
200

Tables

Table 1: Percentage of the occurrence of breeze days/no breeze days at the stations in the period 2006-2015.

	Prevailing Breeze Days (%)					Non-prevailing Breeze Days (%)				
	year	**DJF**	**MAM**	**JJA**	**SON**	**year**	**DJF**	**MAM**	**JJA**	**SON**
Ajaccio	51.9	10.9	66.8	89.1	36.6	48.1	89.1	33.2	10.9	63.4
Bastia	46.5	11.2	56.2	71.7	31.0	53.5	88.8	43.8	28.3	69.0
Solenzara	29.2	0	38.7	55.6	19.6	70.8	100	61.3	44.4	80.4
Pietralba	67.8	49.4	78.7	87.6	49.0	32.2	50.6	21.3	12.4	51.0
Sampolo	75.2	53.4	75.7	88.8	73.1	24.8	46.6	24.3	11.2	26.9